The modeling of tracer exchange and sequestration in the liver[1,2]

CARL A. GORESKY[3]

The McGill University Medical Clinic, Montreal General Hospital, Montreal, Quebec, Canada H3G 1A4

ABSTRACT

Both anatomical and physiological data have been utilized to develop a distributed-in-space mathematical model of the processes of tracer exchange and sequestration in the liver. Comparison with a vascular reference, labeled red cells, indicates that substances entering the freely accessible interstitial or Disse space do so by delayed-wave, flow-limited distribution into that space; lateral or transverse diffusional equilibration occurs virtually instantaneously at each point along the length. In contrast, axial gradients are preserved (lengthwise diffusional equilibration times are orders of magnitude larger than transit times). When a tracer pulse injection is used to explore tracer exchange with liver cells beyond this, the outflow is found to consist of an impulse that is delayed by propagation in the interstitial space and damped by cellular entry (tracer that has not entered liver cells), followed by a reduced-in-magnitude and spread out tailing (tracer that has entered and returned from liver cells). Intracellular metabolic sequestration affects only tracer entering liver cells; it therefore reduces the returning part of the outflow profile. It also results in declining unlabeled substrate axial-concentration gradients in sinusoid and cell, together with a step down in concentration across the liver cell membranes.—**Goresky, C. A.** The modeling of tracer exchange and sequestration in the liver. *Federation Proc.* 43: 154–160; 1984.

The liver is exquisitely designed to facilitate exchange between blood and tissue. Input portal and hepatic arterial vessels supply a hepatic acinus, which consists of radiating plates of hepatic parenchymal cells bathed on each surface by blood perfusing the hepatic sinusoids, the diameter of these being slightly less than that of a red cell. The blood leaves the exchange area via symmetrically distributed terminal hepatic venules. These are distributed in space so that they interdigitate with the input sites. The input and output vessels are never in apposition, so that the structure presents no geometric opportunity for large-vessel diffusional interconnections. The blood flows in the same direction past each face of the hepatic cell plate; the system is thus one in which concurrent flow exists throughout an acinus.

The sinusoid itself has a unique structure. It is lined by flattened endothelial cells, the thin lamella of cytoplasm being pierced by holes of substantial size (the sieve plates) in virtually all areas except those parts occupied by the nucleus. The microvasculature in this organ is thus adapted to promote exchange between the plasma and the interstitium; no substantial barrier exists between the two. The interstitium is a thin lamella behind the sinusoidal lining cells occupied by collagen, ground substance, and occasional reticulin fibers. The parenchymal cells facing this display a multivillar surface; this has evolved in a manner that maximizes the area available for exchange. It is within the confines imposed by this structure that physiological experiments and their interpretation are carried out.

FLOW-LIMITED EXCHANGE IN A DISTRIBUTED SYSTEM

The physiological exchange of materials in the liver has been explored by use of the single-injection, multiple-indicator dilution technique (7). Tracers are used in this approach to elucidate the characteristics of flow in the vasculature, the distribution of materials into the interstitium, and the processes of both cell entry and intracellular disposal. The approach provides information on flow, space sizes, permeabilities, and magnitudes of metabolic processes. The method is nondestructive and interferes in no essential way with organ function. It enables one to carry out the ideal tracer experiment and thus to gain insight into organ function in an undisturbed state. The approach consists of the injection of both the substance to be studied and its appropriate reference (or references); the collection of a series of outflow samples and the assay of these for the injected tracer; the reconstruction from the data of a set of outflow dilution curves (to normalize these, outflow tracer concentrations are divided by the amount of injected tracer activity so that the concentration of each is expressed as an outflow fraction per milliliter); and the interpretation of these normalized outflow tracer profiles by use of a model analysis.

One would expect tracer to be distributed from sinusoidal plasma into its extravascular space in a flow-limited fashion (the sinusoidal barrier will not be expected to limit exchange because of its structure; and, because of the rapidity of diffusion equilibration across dimensions of the order of a capillary radius or hepatocyte half cell width, diffusional equilibration within the extravascular space in a direction transverse

[1] From the Symposium *Kinetics of Capillary Exchange* presented by The American Physiological Society and programed by the Society of Mathematical Biology at the 66th Annual Meeting of the Federation of American Societies for Experimental Biology, New Orleans, Louisiana, April 21, 1982.

[2] Supported by the Medical Research Council of Canada and the Quebec Heart Foundation.

[3] Career Investigator of the Medical Research Council of Canada.

0014-9446/84/0043-0154/$01.25.

to the sinusoidal flow would be expected to occur virtually immediately). Despite these expectations, definition of the flow-limited case evolved slowly at a modeling level. In his studies of inert gas equilibration in or desaturation from tissue (13), Kety defined a flow-limited case in which, at time zero, diffusible label was considered to immediately equilibrate throughout a capillary tissue region, and thereafter to be washed out of the tissue in an exponential fashion. A lumped ordinary differential equation approach was utilized to develop the modeling. Goresky (2), analyzing events in the liver, utilized a distributed-in-space approach to define a kind of flow-limited distribution in which the diffusional expectations outlined above were utilized: in this case equilibration between blood and tissue was envisaged to occur at each point along the length, whereas axial gradients were allowed to develop in sinusoids and tissue along the relatively large distances from entrance to exit. The connection between the two kinds of modeling became clear when Perl and Chinard (14) considered the case in which axial diffusion was allowed to become infinitely rapid, in which, despite the length of the capillary tissue units, equilibration was envisaged to occur immediately from entrance to exit. The capillary tissue unit then behaved like a capacitor, reproducing the behavior of the Kety model. The problem with this kind of washout model is that anatomical distances in the axial direction are much too large for diffusional equilibration to occur in that direction. Expected axial equilibration times are many orders of magnitude larger than capillary transit times. The Kety model then cannot exist in the form described. The kind of flow-limited distribution expected to occur in a physiological system is the delayed-wave, flow-limited distribution described by Goresky (2).

Now let us derive the conservation relation for the system by utilizing the schema illustrated in Fig. 1. At a time t consider the material in the vascular space in the segment n of length Δx that lies opposite the extravascular segment m. Let this material be transported to the right by flow so that it now lies opposite the segment $m + 1$ and let it remain there and exchange for the time Δt. In algebraic fashion, let $u(x,t)$ be the concentration at the place x and time t in the vascular space (in which flow occurs); $v(x,t)$, the concentration in the adjacent extravascular space; A, the volume per unit length of the vascular space;

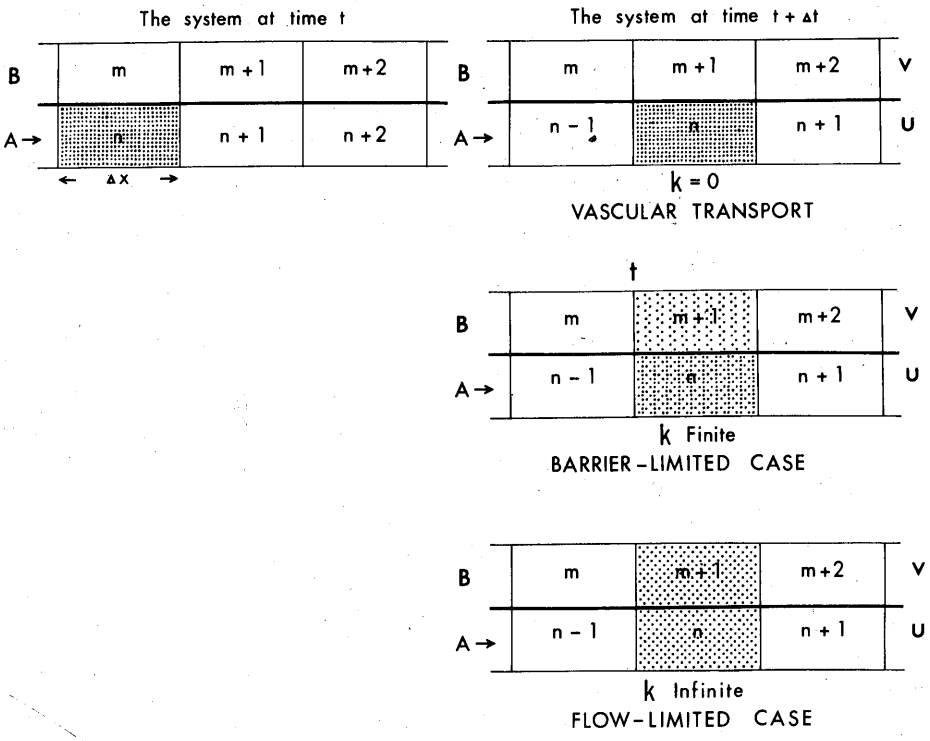

Figure 1. Schematic illustration of events in a distributed system. In the left-hand panel tracer is introduced into an element of the vascular compartment at the time t. The material in each element in this vascular compartment is then allowed to flow the distance Δx to the right and to remain in that position for the time Δt. During this time exchange will occur with the adjacent extravascular compartment at a rate determined by the rate constant k. When the barrier is impermeable ($k = 0$), the tracer will flow with the fluid; when it is poorly permeable (k finite), equilibration will not be reached before flow once again transports the vascular fluid to the right; and when the barrier is freely permeable (k infinite), equilibration occurs between the vascular and extravascular spaces. The latter corresponds to the flow-limited case. From ref 11. © 1970 Munksgaard International Publishers Ltd., Copenhagen, Denmark.

and B, the corresponding volume per unit length of the extravascular space. Then

$$u(x - \Delta x,t)A\Delta x = u(x,t + \Delta t)A\Delta x + v(x,t + \Delta t)B\Delta x - v(x,t)B\Delta x$$

or

$$B[v(x,t + \Delta t) - v(x,t)]\Delta x = -A[u(x,t + \Delta t) - u(x - \Delta x,t)]\Delta x = -A[u(x,t + \Delta t) - u(x,t) + u(x,t) - u(x - \Delta x,t)]\Delta x$$

and so

$$B\left[\frac{v(x,t + \Delta t) - v(x,t)}{\Delta t}\right] = -A\left\{\frac{u(x,t + \Delta t) - u(x,t)}{\Delta t} + \frac{[u(x,t) - u(x - \Delta x,t)]\Delta x}{\Delta t\Delta x}\right\}$$

Now let $\Delta x/\Delta t = W$, velocity of flow. Then, in the limit Δx, $\Delta t \to 0$,

$$B\frac{\partial v}{\partial t} = -A\left(\frac{\partial u}{\partial t} + W\frac{\partial u}{\partial x}\right)$$

Then, if $\gamma = B/A$, the ratio of the volumes per unit length, the conservation equation becomes

$$\gamma\frac{\partial v}{\partial t} + \frac{\partial u}{\partial t} + W\frac{\partial u}{\partial x} = 0 \qquad (1)$$

Now incorporate our diffusional expectations. In the small dimensional extreme (in the direction transverse to flow), diffusional equilibration will occur so rapidly at each point along the length that we may set

$$v(x,t) = u(x,t) \qquad (2a)$$

and

$$\frac{\partial v}{\partial t} = \frac{\partial u}{\partial t} \qquad (2b)$$

so that

$$\frac{1 + \gamma}{W}\frac{\partial u}{\partial t} + \frac{\partial u}{\partial x} = 0 \qquad (3)$$

Now, at time $t = 0$, introduce in the

initially empty system an impulse input at the origin

$$u(x,0) = \frac{q_0}{A}\,\delta(x) = \frac{q_0}{F_s}\,\delta\left(\frac{x}{W}\right)$$

where q_0 is the amount of tracer injected, F_s is the sinusoidal flow ($F_s = AW$), and $\delta(x)$ is a Dirac delta function at the origin. Then, from this we find

$$u(x,t) = \frac{q_0}{F_s}\,\delta\left[t - (1+\gamma)\,\frac{x}{W}\right] \quad (4)$$

The injected impulse behaves like a delayed wave. If the vascular reference travels with a velocity W, the diffusible substance travels with the velocity $W/(1+\gamma)$. The impulse in each case remains compact in space; it does not become dispersed. The diffusible tracer bolus travels more slowly, the degree of retardation depending on its accessible extravascular volume of distribution.

Because the focus of this symposium is the mathematical modeling of exchange processes between blood and tissue, events at the level of the single sinusoid will be emphasized. At the same time, to provide continuity at the physiological level, it is appropriate to illustrate how the delayed-wave phenomenon has been utilized at the level of interpreting the information available in whole-organ hepatic outflow dilution curves. A set of outflow compartment label dilution curves is illustrated in Fig. 2 (the probes injected included ^{51}Cr-labeled red cells, a vascular reference; T-1824-labeled albumin, which is confined to the capillary space during a single passage in organs with a nonfenestrated capillary endothelium; ^{14}C-labeled sucrose, a classical extracellular space label; and ^{3}H-labeled water, which would be expected to penetrate liver cells fairly freely). The curves exhibit a progressive shape change from one to another; in terms of the whole sequence, there is a progressive delay of outflow appearance, a diminution in the rate of rise, a depression in the peak outflow fraction per milliliter, and a decreased rate of downslope decay.

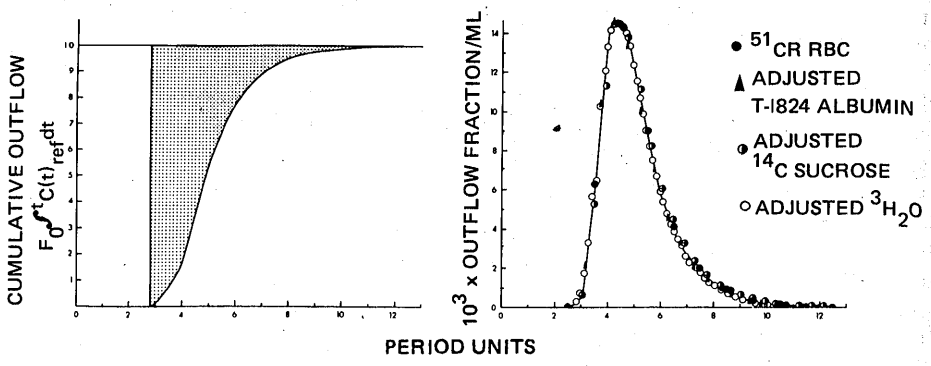

Figure 3. The left-hand panel illustrates the relation between the calculated common large-vessel transit time and the cumulative outflow of the reference substance. The shaded area corresponds to the distribution of sinusoidal transit times. The right-hand panel illustrates the superimposition of the adjusted diffusible label curves on the labeled red cell curves. The data correspond to those illustrated in Fig. 2. From ref 3.

Each indicator appearing at the outflow passes through both large (nonexchanging) and sinusoidal (exchanging) vessels. A variety of relations between these are possible, depending on the structure of the network and the kind of flow coupling. The circulation of the liver lies at an extreme in this possible spectrum (12, 15): the distribution of outflow transit times appears to arise almost completely from the distribution of exchanging vessel transit times. With this kind of relation between large-vessel and small-vessel transit times, one would expect from the delayed-wave modeling that after a common large-vessel transit time, the differences between the outflow curves for the various substances undergoing delayed-wave, flow-limited distribution could be described by the differences in a single parameter γ, the ratio of the extravascular to intravascular spaces of distribution for the tracer concerned. Reversal of the flow-limited delay effect (by decreasing the sinusoidal transit, after a common large-vessel transit time, by the ratio $1/(1+\gamma)$, and by simultaneously increasing the tracer concentration by the reciprocal of this factor to preserve the experimental outflow area) will be expected to result in superimposition of each adjusted diffusible label outflow curve on the vascular label, the labeled red cell curve (2). This is indeed what occurs (see Fig. 3). All the diffusible label curves superimpose indistinguishably on the labeled red cell curve. The strength of the argument lies not only in the individual transformations but also in the superposition of the whole set of curves after a common initial transit time. No other set of premises has been found to explain this; the effect persists even after the distortion imposed by collection through a catheter system (10).

The data also indicate that labeled albumin, as well as the labeled sucrose, penetrates the interstitial space, but that it enters only some of the space. This characteristic exclusion of labeled albumin from part of the interstitium, which is now known to occur in most other organs, was first demonstrated in vivo in the liver (2). The exclusion phenomenon was immediately visible in this organ because the interstitium is essentially directly exposed to the plasma at the level of the sinusoid. The labeled water curves were found to form an extension of the spectrum encompassing the interstitial materials. The labeled water undergoes flow-limited distribution into the liver cells; it provides an

Figure 2. Hepatic venous outflow dilution curves. The ordinate on the left-hand panel is semilogarithmic; and that on the right, linear. The duration of a collection period was 1.67 s. From ref 3.

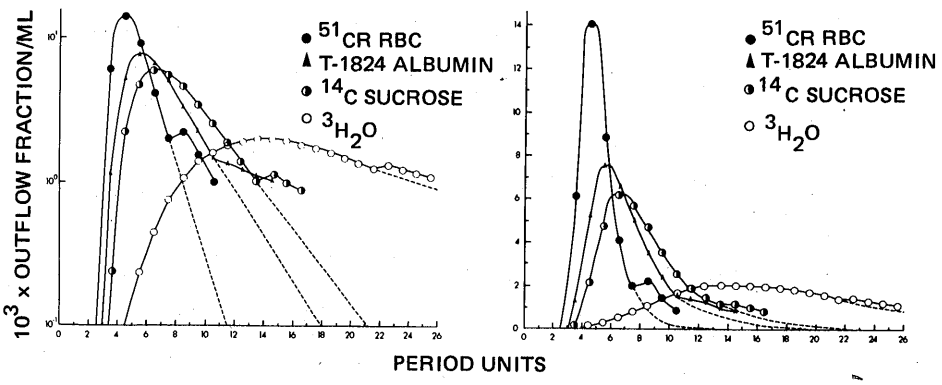

asymptotic extreme to which materials not freely entering liver cells may be compared.

The flow-limited transformation developed for the liver has also been found to fit labeled water curves in the lungs (6). The extravascular space ordinarily available to labeled water in the lungs is relatively small (the air spaces are large), and the relative displacement of the water curve from the reference is small. In the absence of flow-limited distribution of the interstitial materials (they are distributed in a barrier-limited fashion in the lungs), the nagging question remained of whether, despite the transformation, labeled water could be partly barrier-limited in its distribution in this organ. The flow-limited character of the distribution has now been confirmed in the lungs in a different fashion: Chinard and DeFouw (1) have shown that when the alveolar spaces are filled with isotonic fluid (so that it is not immediately reabsorbed), a flow-limited kind of curve is again found, this time corresponding to a much larger space. The labeled water permeability is so large that it does not limit tracer entry into the larger space. In other organs (the heart, for instance), where the large-vessel and capillary transit times increase together (15), flow-limited outflow profiles will be described differently.

TRACER EXCHANGE BETWEEN LIVER CELLS AND PLASMA

The principles underlying tracer exchange between cells and their surrounding milieu have been developed by studying tracer exchange in isolated cell suspensions. In general, substrate exchange between cell and medium has been found to vary with the concentration in each space (in particular, the unidirectional flux out of each compartment is a function of the concentration in that compartment). The concentrations in the two compartments are intensive properties of the system. The transfer across a cell membrane separating an intracellular space from an extracellular environment has been found to depend on the permeability and surface area of the membrane as well as the concentrations on either side. The volumes of the spaces on each side of the membrane are extensive properties of the system and are important only in that they enable one to describe the conservation relation. If the membrane transferring mechanism is linear, the apparent permeability will not change as a function of concentration, whereas if it depends on the amount of a carrier material in the membrane, it may saturate at higher concentrations (the process may become nonlinear).

The equations describing cellular exchange in a distributed-in-space sinusoid cell system can be developed from elementary principles, as for the initial flow-limited case (see Fig. 4). Once again let flow-limited exchange occur between plasma and interstitium. Consider that, superimposed on this, there is a barrier-limited exchange process between the interstitium and the intracellular compartment. Let $z(x,t)$ represent the tracer concentration in the cells distributed along the length; C is defined as the volume per unit length of cellular compartment; and $C/A = \theta$ is the (cellular/sinusoidal plasma) space ratio. Then, for the conservation relation, we find the following equation:

$$\frac{1+\gamma}{W}\frac{\partial u}{\partial t} + \frac{\partial u}{\partial x} + \frac{\theta}{W}\frac{\partial z}{\partial t} = 0 \qquad (5)$$

This must be solved together with the equation describing cellular exchange, which may be cast as follows,

$$C\frac{\partial z}{\partial t} = k'_1 S_c u - k'_2 S_c z \qquad (6a)$$

where k'_1 and k'_2 are permeability-type cell entry and exit constants, respectively, and S_c is the cellular surface area per unit length. This equation may also be expressed in a more compact form:

$$\frac{\partial z}{\partial t} = \frac{k'_1 S_c}{C} u - \frac{k'_2 S_c}{C} z = k_1 u - k_2 z \qquad (6b)$$

where now $k_1 = k'_1 S_c/C$ and $k_2 = k'_2 S_c/C$. The solutions (4) to this set of equations, in space and time, in response to an impulse input at $x = 0$ and $t = 0$ in an initially empty system, are

$$u(x,t) = \frac{q_0}{F_s} e^{-k_1\theta x/W} S\left[t - (1+\gamma)\frac{x}{W}\right] + \frac{q_0}{F_s} e^{-k_1\theta x/W} e^{-k_2[t-(1+\gamma)x/W]} \sqrt{\frac{f}{g}} \times I_1(2\sqrt{fg}) S\left[t - (1+\gamma)\frac{x}{W}\right] \qquad (7a)$$

and

$$z(x,t) = \frac{q_0}{F_s} k_1 e^{-k_1\theta x/W} e^{-k_2[t-(1+\gamma)x/W]} \times I_0(2\sqrt{fg}) S\left[t - (1+\gamma)\frac{x}{W}\right] \qquad (7b)$$

where $f = k_1\theta k_2 x/W$, $g = t - (1+\gamma)x/W$, and $S(t-a)$ is a step function at $t = a$. An implicit assumption in the

Figure 4. Schematic illustration of the modeling of cellular exchange, and of cellular exchange with sequestration, in the liver sinusoid cell system when a barrier-limiting process (transport-mediated cell entry is one of these) is situated at the cell membrane. The rate constants k_1, k_2, and k_3 are those for cell entry, efflux, and sequestration, respectively. From ref 3.

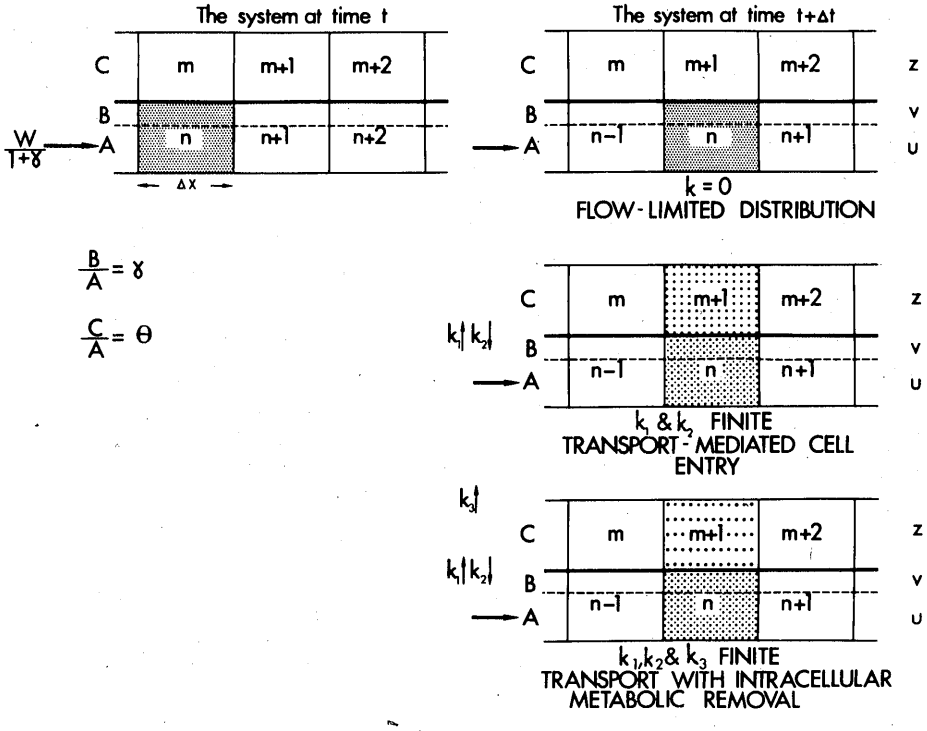

physiological use of this kind of tracer experiment is usually that there is an underlying steady-state distribution of the unlabeled substrate. The tracer experiment then provides kinetic information concerning the size of the cellular space available to substrate and the rate of distribution of tracer into that space. The underlying concentration steady state can be explored either by analyzing tissue, knowing the volumes of the various compartments, or by utilizing a prolonged steady infusion of tracer. In either instance, in the absence of intracellular sequestration, the steady state is one in which concentrations from input to output (both for bulk and tracer) will be the same, and in which

$$z(x,t) = (k_1/k_2)u(x,t) \qquad (8)$$

When $k_1/k_2 \gg 1$, the membrane transfer process is highly concentrative (4); when $k_1/k_2 = 1$, it is nonconcentrative (9).

Equations 7a and *7b* describe the way in which tracer disperses within the underlying steady state as a function of both position and time. The impulse propagates along the sinusoid with the retarded velocity $W/(1 + \gamma)$, loading the tissue. Behind it, the activity in the tissue returns to the plasma to form a trailing plasma concentration profile. Figure 5 portrays these events at various times as a function of length along the sinusoid. A labeled red cell (the vertical dashed line) propagates with flow and emerges at a normalized transit time of 1.0. The labeled impulse function, the solid vertical line, is excluded from the cell; it propagates in both the vascular and interstitial spaces. In this case, where $\gamma = 1$, it propagates half as fast as the labeled red cell and emerges at the normalized time 2.0. The proportion of the initial label in the impulse decreases exponentially along the length (in this case to 0.549 at the outflow) by virtue of its loss to the adjacent cells during passage. The dashed horizontal profile, trailing behind the impulse, portrays the tissue concentration. The adjacent solid trailing intravascular profiles have been calculated for two cases: for a nonconcentrative uptake process ($k_1/k_2 = 1.0$), the upper profile; and for a concentrative uptake process ($k_1/k_2 = 6.0$), the lower profile. In the concentrative case, the label is held within the cell for a much longer time.

Events within the tissue will usually be inaccessible to the physiologist; rather, outflow profiles will be available. In Fig. 6, single sinusoidal outflow profiles are displayed: on the left, for the concentrative case, and on the right, for the nonconcentrative case. The labeled red cell (the dash-dot vertical line) emerges at a normalized transit time of 1.0. The damped tracer impulse (the solid vertical line), which consists of tracer that has never entered the liver cells, emerges at a normalized transit time of 2.0. This is followed in each case by a trailing profile, which consists of tracer that has entered and then left the liver cells. When concentrative uptake is taking place, the trailing profile is initially lower in magnitude than it is in the nonconcentrative case; it is also more spread out in time. As the permeability of the liver cell surface increases, the proportion of label in the initial impulse function diminishes until, finally, virtually all of the label emerges in the delayed trailing profile. With a further increase in the permeability, this profile is reshaped, becoming more compact, until in the infinite permeability extreme it emerges as an impulse function at a time corresponding to its volume of distribution. We would expect the high-permeability asymptote to be represented by labeled water in the nonconcentrative case.

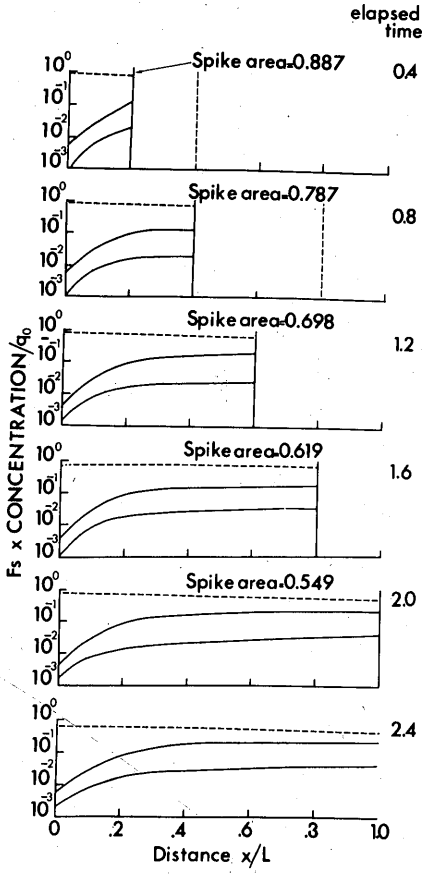

Figure 5. Tracer concentration-space profiles in the sinusoids and the liver cells at various times after an impulse at the origin at $t = 0$. Tracer exchange but not sequestration is taking place. From ref 8.

The single sinusoid modeling illustrates the principles underlying tracer exchange between liver sinusoids and liver cells. These have then been utilized at the level of whole-organ experiments. At a practical level, the inferences arising from the modeling have been utilized in experimental design. The injection mixture has been designed to include not only labeled red cells and the tracer substrate being studied, but also a second reference that does not enter the liver cells, one of molecular weight similar to the tracer that undergoes interstitial flow-limited distribution in the fashion expected of the tracer substrate if it did not enter the liver cells. At an interpretive level, the model analysis has been utilized to study the exchange of labeled rubidium (4), a highly concentrative process, and that of labeled glucose, a nonconcentrative process (9). In the analysis, the outflow profile automatically separates into two parts: the throughput components, which arise from the delayed and damped tracer impulse function, and the exchanging components, which represent material that has entered the liver cells, to later return to the circulation.

THE SEQUESTRATION OF TRACER ENTERING LIVER CELLS

The irreversible removal of tracer (and of bulk) within the liver cells creates a whole new set of circumstances. The outflow recovery of tracer is reduced, and an underlying concentration steady state for unlabeled substrates is established in which falling concentration gradients are present, both within sinusoids and within cells, from input to output.

We now define k_3 as an intracellular sequestration rate constant, with the dimensions milliliter second^{-1} (milliliter intracellular volume)$^{-1}$. The equation of conservation for the intracellular removal case (Fig. 4) then becomes

$$(1 + \gamma)\frac{\partial u}{\partial t} + \frac{\partial u}{\partial x} + \frac{\theta}{W}\frac{\partial z}{\partial t} + \frac{k_3\theta}{W}z = 0 \qquad (9)$$

The equation describing the combined

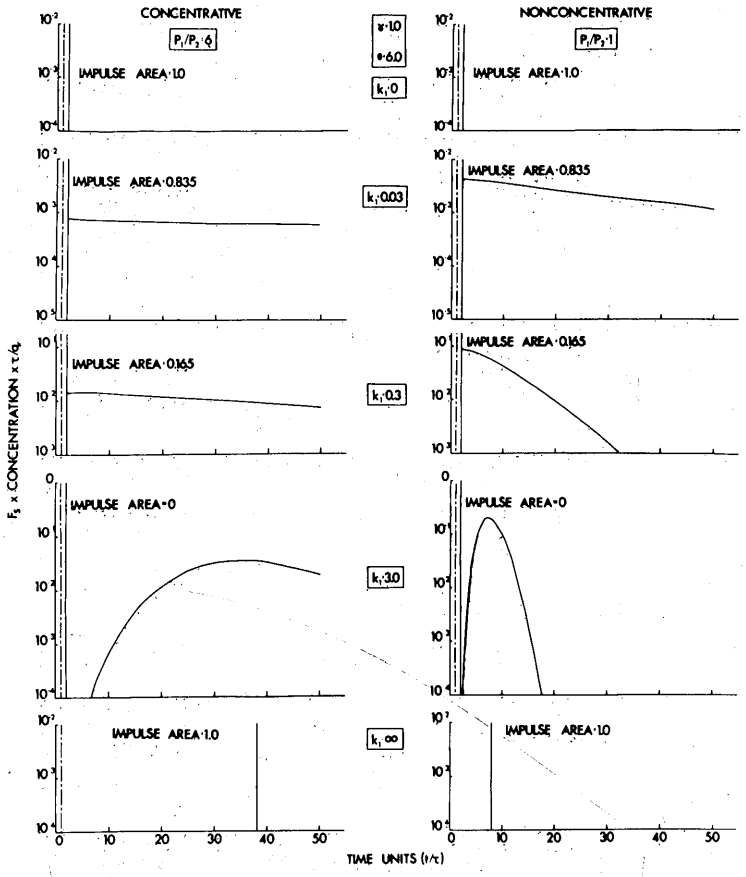

Figure 6. Tracer outflow concentration-time profiles corresponding to the example illustrations of Fig. 5. From ref 8.

effects of exchange across the cell membrane and of intracellular sequestration is

$$\frac{\partial z}{\partial t} = k_1 u - k_2 z - k_3 z \qquad (10)$$

The solutions to this set of equations, in response to an impulse input at $x = 0$ and $t = 0$, in an initially empty system, are (5)

$$u(x,t) = \frac{q_0}{F_s} e^{-k_1\theta x/W} \delta\left[t - (1+\gamma)\frac{x}{W}\right]$$

$$+ \frac{q_0}{F_s} e^{-k_3[t-(1+\gamma)x/W]} e^{-k_1\theta x/W} e^{-k_2[t-(1+\gamma)x/W]}$$

$$\times \sqrt{\frac{f}{g}} I_1(2\sqrt{fg}) S\left[t - (1+\gamma)\frac{x}{W}\right] \qquad (11a)$$

and

$$z(x,t) = \frac{q_0}{F_s} e^{-k_3[t-(1+\gamma)x/W]} e^{-k_1\theta x/W} e^{-k_2[t-(1+\gamma)x/W]}$$

$$\times I_0(2\sqrt{fg}) S\left[t - (1+\gamma)\frac{x}{W}\right] \qquad (11b)$$

where once again $f = k_1\theta k_2 x/W$ and $g = t - (1+\gamma)x/W$.

The effect of intracellular sequestration on tracer kinetics is best explored by comparing the label removal profiles with those that would occur if no removal process were present (by comparing *Eqs. 11a* and *11b* with *Eqs. 7a* and *7b*). A new exponential removal function, $\exp\{-k_3[t-(1+\gamma)x/W]\}$, appears in the second or returning term of $u(x,t)$, and in the expression for $z(x,t)$. At an illustrative level, a set of spatial profiles is displayed in Fig. 7, corresponding to those previously shown for the nonconcentrative ($k_1/k_2 = 1.0$) case. The shaded areas illustrate the fashion in which sequestration reduces the trailing intracellular and intravascular profiles. The delayed and damped intravascular tracer impulse propagates to the outflow, unaffected by the sequestration (this is expected because the outflowing impulse consists of tracer that never entered the liver cells, and has never been exposed to the sequestration process). Tracer outflow curves corresponding to this are presented in Fig. 8. One can see the dramatic removal effects on the later trailing parts of the outflow profile (shading is used once again to highlight the effect of the removal process). At a theoretical level the cumulative predicted outflow recovery of tracer, in relation to the injected amount q_0, is $q_0 \times \exp[-k_1\theta k_3\tau/(k_2+k_3)]$, where $\tau = x/W$, the vascular transit time (that for a labeled red cell). If both the membrane exchange process and the metabolic sequestration step are linear, one can extrapolate directly to the underlying unlabeled substrate concentration profile by examining the solutions to *Eqs. 9* and *10* at long time, in response to a steady infusion. If the two corresponding parent unlabeled species are u_{par} and z_{par}, the description of the underlying profile is found to be

$$u_{par}(x) = u_{par}(0) \exp\left(-\frac{k_1\theta k_3}{k_2+k_3}\frac{x}{W}\right) \qquad (12a)$$

and

$$z_{par}(x) = \frac{k_1}{k_2+k_3} u_{par}(x) \qquad (12b)$$

The predicted lengthwise (or axial) concentration profiles (5) are exponential:

Figure 7. Tracer concentration space profiles, where intracellular sequestration is occurring. The shaded areas illustrate the removal effect. In this case $k_3 = 0.10$ ml·s^{-1}·(ml intracellular space)$^{-1}$. From ref 8.

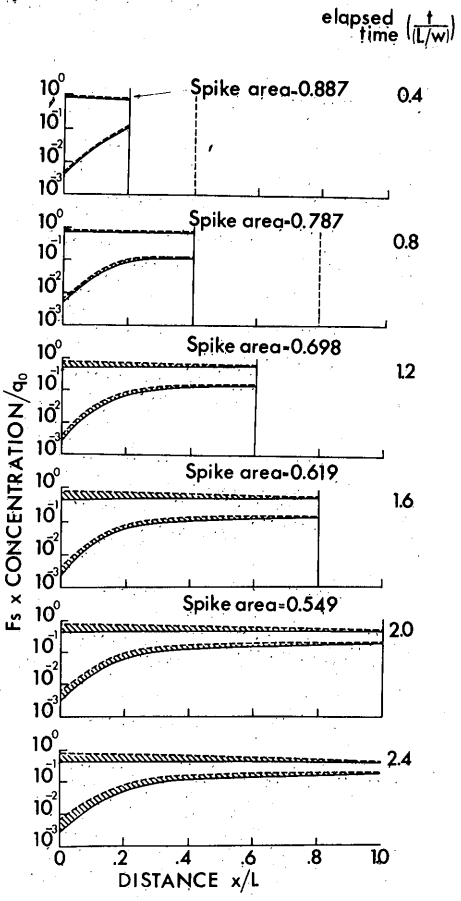

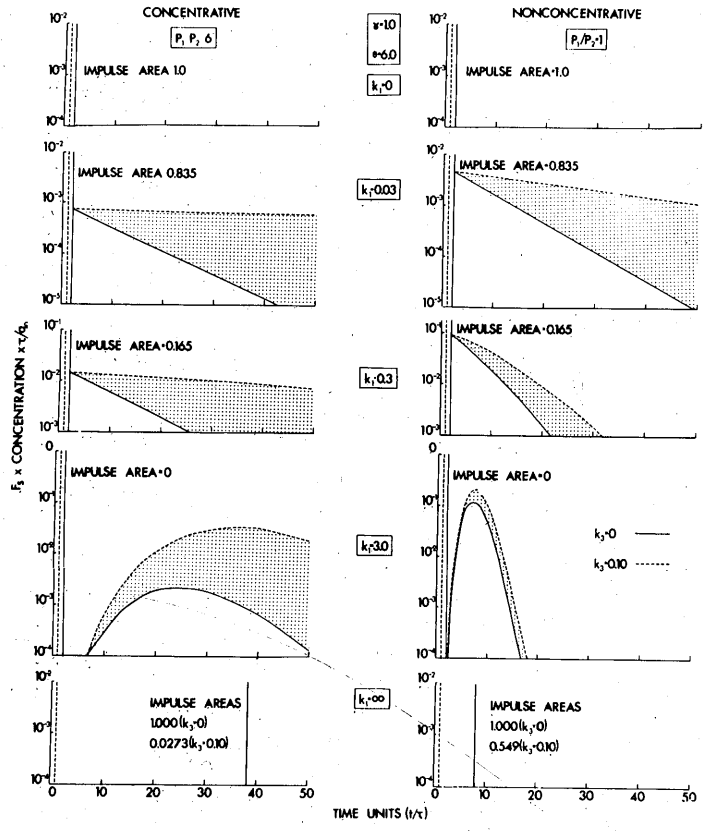

Figure 8. Tracer outflow concentration time profiles corresponding to the example illustrations of Fig. 7. The shaded areas once again highlight the removal effect. From ref 8.

that for the intravascular concentration predicts that the outflow recovery of the unlabeled parent will match that expected for the labeled substrate, and that for the intracellular concentration profile indicates that, in addition to the exponential profile, there is a step down in concentration across the cell membrane, from plasma to cell space; cellular concentrations are everywhere lower than corresponding intravascular concentrations.

The metabolic sequestration modeling has been extended to whole-organ data in the analysis of a set of labeled galactose outflow dilution curves (5). Estimates of not only membrane rate constants but also metabolic sequestration constants have been obtained. The analysis indicates that it is possible, in an intact undisturbed organ, to separate and quantitate the limiting processes at the two levels (membrane transfer and intracellular metabolism) by virtue of the analysis of tracer outflow data. Moreover, the analysis takes into account the distributed-in-space aspects of the process and the effects of the underlying axial concentration gradients. It lays the basis for a new in vivo approach to metabolic events within the liver. FP

REFERENCES

1. **Chinard, F. P.; DeFouw, D. W.** Pulmonary transport of water and solutes: functional and structural correlations. *Federation Proc.* 42: 2435–2439; 1983.
2. **Goresky, C. A.** A linear method for determining liver sinusoidal and extravascular volumes. *Am. J. Physiol.* 204: 626–640; 1963.
3. **Goresky, C. A.; Bach, G. G.** Membrane transport and the hepatic circulation. *Ann. N.Y. Acad. Sci.* 170: 18–47; 1970.
4. **Goresky, C. A.; Bach, G. G.; Nadeau, B. E.** On the uptake of materials by the intact liver: the concentrative transport of rubidium-86. *J. Clin. Invest.* 52: 975–990; 1973.
5. **Goresky, C. A.; Bach, G. G.; Nadeau, B. E.** On the uptake of materials by the intact liver: the transport and net removal of galactose. *J. Clin. Invest.* 52: 991–1009; 1973.
6. **Goresky, C. A.; Cronin, R. F. P.; Wangel, B. E.** Indicator dilution measurements of extravascular water in the lungs. *J. Clin. Invest.* 48: 487–501; 1969.
7. **Goresky, C. A.; Groom, A.** Microcirculatory events in the liver and the spleen. Renkin, E. M.; Michel, C.; Geiger, S., eds. *Handbook of physiology, Section II, The cardiovascular system, Vol. 4, The microcirculation.* Bethesda: Am. Physiol. Soc. In press.
8. **Goresky, C. A.; Huet, P.-M.; Villeneuve, J. P.** Blood-tissue exchange and blood flow in the liver. Zakim, D.; Boyer, T. D., eds. *Hepatology.* Philadelphia: Saunders; 1982: 32–63.
9. **Goresky, C. A.; Nadeau, B. E.** Uptake of materials by the intact liver: the exchange of glucose across the cell membranes. *J. Clin. Invest.* 53: 634–646; 1974.
10. **Goresky, C. A.; Silverman, M.** Effect of correction of catheter distortion on calculated liver sinusoidal volumes. *Am. J. Physiol.* 207: 883–892; 1962.
11. **Goresky, C. A.; Ziegler, W. H.; Bach, G. G.** Barrier-limited distribution of diffusible substances from the capillaries in a well perfused organ. Crone, C.; Lassen, N. A., eds. *Capillary permeability.* Copenhagen: Munksgaard; 1970: 171–184.
12. **Goresky, C. A.; Ziegler, W. H.; Bach, G. G.** Capillary exchange modeling; barrier-limited and flow-limited distribution. *Circ. Res.* 27: 739–764; 1970.
13. **Kety, S. S.** Theory and applications of the exchange of inert gas at the lungs and tissues. *Pharmacol. Rev.* 3: 1–41; 1951.
14. **Perl, W.; Chinard, F. P.** Convection diffusion model of indicator transport through an organ. *Circ. Res.* 22: 273–298; 1968.
15. **Rose, C. P.; Goresky, C. A.** Vasomotor control of capillary transit time heterogeneity in the coronary circulation. *Circ. Res.* 39: 541–554; 1976.